

PROPAGATION OF CHARGED PARTICLE BEAMS IN THE ATMOSPHERE\*

Martin Lampe  
 Plasma Theory Branch, Code 4792  
 Naval Research Laboratory  
 Washington, D. C. 20375-5000

Abstract

We shall review the basic physical processes involved in charged particle beam propagation, in a self-pinched mode, in the atmosphere or other dense neutral gases. These processes include single-particle collisional and radiative energy losses, collective energy loss, radial expansion due to scattering, and instabilities. Each of these imposes requirements and limitations on beam propagation. We shall concentrate on highly relativistic electron beams. Ion beam physics is similar but more complex (because ultra-relativistic approximations are inappropriate), and has been less studied.

Introduction

A charged particle beam injected into a neutral gas begins immediately to ionize the gas. For example, in air at standard atmospheric density each beam electron collisionally ionizes about 100 thermal electrons per cm. Thus, the "plasma" electron density  $n$  exceeds the beam density  $n_b$  almost immediately. Over a time scale  $1/4\pi\sigma$ , a very strong radial space charge field expels a small fraction of the plasma electrons, thereby setting up a charge-neutral region within the beam and out to a large radius  $b=c/4\pi\sigma$ . (Since the plasma is typically weakly ionized and collisional, it can be characterized by a local scalar conductivity  $\sigma$ .) Thereafter, the only radial forces on the beam are magnetic: the beam is pinched by its self-force, but this may be partially neutralized by reverse currents induced in the plasma. The beam thus propagates in a self-pinched equilibrium, with the magnetic pinch balancing the beam's transverse pressure, as well as any centrifugal force if the beam is rotating. The equilibrium radius is proportional to the emittance and inversely proportional to the net (beam plus plasma) current  $I_n$ . (If the radial profile of the plasma current  $J(r)$  differs from that of beam current  $J_b(r)$  it is necessary to define an appropriate radially-averaged "effective current" that controls the pinch strength [1]. We shall neglect such subtleties here.) Since  $I_n$  generally increases as one moves backward in the beam, the equilibrium has a trumpet-like appearance, with the radius steadily decreasing (Fig. 1a). Indeed, the very front of the beam, where charge neutrality has not been established, is unpinched, has a large radius and constantly erodes due to both radial expansion and energy loss.

Single-Particle Energy Loss

Highly relativistic electrons lose energy, due to ionizing collisions with gas atoms, at a rate given by Bethe's formula [2,3],

$$dE/dz = -(2\pi n Z e^4 / mc^2) \ln(\gamma^3 m^2 c^4 / 2n^2 \langle \omega \rangle^2), \quad (1)$$

where  $n$  is the gas atom number density,  $Z$  the atomic number, and  $\langle \omega \rangle$  a characteristic bound electron energy. For electrons with  $E \geq 1$  MeV in full-density air, this stopping power is 200 to 300 keV/m.

For high-energy electrons (e.g.,  $\geq 100$  MeV in air), energy loss due to bremsstrahlung emission dominates. This energy loss process proceeds exponentially, with the mean energy  $\langle E \rangle$  decreasing as

$$d\langle E \rangle / dz = -\langle E \rangle / \lambda_r, \quad (2)$$

with the radiation length  $\lambda_r$  given by

$$1/\lambda_r = 4nZ(Z+1)(e^2/\hbar c)(e^2/mc^2)^2 \ln \Lambda, \quad (3)$$

with  $\Lambda = 192/Z^{1/3}$  if  $\gamma \geq 100$ , or  $\Lambda = \gamma$  if  $\gamma < 100$ . In standard-density air,  $\lambda_r \approx 300$ m. Bremsstrahlung energy loss is statistical in nature, leading to a large energy spread ("straggling"). This has important implications for beam stability and range [4].

Other single-particle energy loss mechanisms, e.g., synchrotron radiation, are relatively unimportant for beams propagating in air.

Radial Expansion

As a result of multiple small-angle scattering off nuclei, an unpinched electron beam in standard-density air expands as the  $3/2$  power of distance. This expansion is rapid as compared to energy loss. A pinched beam also expands as its emittance increases by scattering, but in a different and much slower way. Energy loss also has an effect on the beam radius  $a$ .

Let us consider a beam which is subject to the energy loss mechanisms discussed above, as well as to multiple small-angle scattering at an angular rate [2]

$$S = d\langle \theta^2 \rangle / dz = 16\pi n (Ze^2/\gamma mc^2)^2 \ln(210/Z^{1/3}). \quad (4)$$

Because neither electron-electron collisions nor bremsstrahlung emission result in angular scattering of a high-energy electron (to within order  $1/\gamma$ , assumed negligible), it is easily seen that these mechanisms leave the unnormalized emittance  $\epsilon = a \sqrt{\langle \theta^2 \rangle}$  invariant. If we assume that scattering is slow compared to a betatron oscillation wavelength  $\lambda_B$  of the beam electrons in the pinch potential, i.e., that  $\lambda_B S / \langle \theta^2 \rangle \ll 1$ , it can be shown [5] that the beam radial profile assumes a self-similar Bennett profile, and that  $\epsilon^2$  increases at a rate  $a^2 S$ . In equilibrium,  $\langle \theta^2 \rangle$  is fixed by Bennett condition,

$$\langle \theta^2 \rangle = I_n / I_A, \quad (5)$$

where  $I_A = 17\beta\gamma$  kA is the Alfvén-Lawson current. Thus, the slow changes in  $\gamma$  (energy loss) and  $\epsilon$  (scattering) lead to a steady adiabatic change in  $a$ ,

$$d \ln(\gamma^{-1/2} I_n^{1/2} a) / dz = 1/L_N, \quad (6a)$$

where

$$L_N = (\hbar c / 2\pi e^2) (I_n / I_A) \gamma^2 \lambda_r. \quad (7)$$

For example,  $L_N = (I_n E / 7 \times 10^{12} \text{ watts}) \lambda_r$  in standard density air. Equations (6), (7) are known as the Nordsieck equation, derived in its basic form (but never published) by A. Nordsieck in the early 1960s. Later contributions were made by Lee [5,6]. Fawley (unpublished recent work) was the first to derive the correct energy dependence in the LHS of (6a). (unpublished).

Energy loss that is due to the effect of  $E_n$  electric fields (ohmic loss, to be discussed below) conserves the transverse momentum  $p_{\perp} = \gamma m v_{\perp}$  of each beam electron, and thus, increases the transverse pressure  $\langle \gamma n_{\perp} m v_{\perp}^2 \rangle$ . Ohmic energy loss thus causes beam expansion, whereas it is evident in Eq. (6a) that single-particle energy loss leads to beam contraction. Mathematically, it can be shown that ohmic loss leaves the normalized emittance  $\gamma \epsilon$  constant, and that when it predominates the Nordsieck equation takes the form

$$d \ln(\gamma^{1/2} I_n^{1/2} a) / dz = 1/L_N. \quad (6b)$$

A few electrons undergo larger-angle single scatterings, which lead to "Moliere scattering" [7]. These electrons escape to large radius, and it is simplest to regard them as lost. This leads to a slow decrease in beam current  $I_b$ , but to a reduced rate of emittance growth for the remaining beam. The net effect [8] is to increase  $L_N$  by 20% to 40%, which is in good agreement with experiment [9].

A beam can only be considered to be pinched, and the Nordsieck equation only applies, if the Nordsieck expansion rate (basically an exponential process with e-folding range  $L_N$ ) is slower than the diffusive expansion rate for an unpinched beam. This sets a minimum condition for propagation in the pinched mode in a dense medium. It is also to be noted that in air Nordsieck expansion occurs more rapidly than single-particle energy loss if  $I < 80kA$  and  $E < 100MeV$ , or if  $I E < 7 \times 10^{12}$  watts and  $E > 100MeV$ . It is thus evident that high current and/or energy are necessary for effective self-pinched propagation in dense media.

Energy loss and radial expansion represent fundamental limitations on range, which can be alleviated only by propagating in a reduced-density channel ("hole-boring"). This can be accomplished by sacrificing the front of a particle beam to heat the air and induce radial expansion, which increases the range of the beam tail, or by using a series of beam pulses to produce the same effect, or by using some other means to heat and prepare a reduced-density channel.

Plasma Return Current, Ohmic Loss, and Nose Erosion

Lenz's law suggests that a CPB should induce an axial electric field  $E_z$  which opposes the propagation of the beam and drives a reverse current in the conducting medium.  $E_z$  extracts energy from the beam and eventually dissipates it in the plasma through resistive decay of the return current. For a highly relativistic beam with  $v \approx c$ ,  $E_z$  does not arise at the very front of the beam, where the gas is non-conducting. The fields there are purely transverse electrostatic/magnetostatic. In effect, the beam serves as a guide for an electromagnetic wave ( $E_r, B_\theta$ ) in the vacuum. As  $\sigma$  increases, many things happen in rapid succession at the point where  $\zeta = ct - z = c/4\pi\sigma$ . ( $\zeta$  is the distance behind the beam head, a very useful coordinate for many purposes.) The beam charge is neutralized and the self-pinch is established. (Hence, this region of the beam is called the "pinch point".) Maxwell's equations reduce to Ampere's law out to the radius wherein space charge neutrality prevails. The  $E_r$  field "turns around" and becomes an  $E_z$  field which is governed by the inductive term in Ampere's law. This leads to a very large spike in the field  $E_z(z)$ , which can reach many MV/m. As  $\sigma$  continues to increase rapidly, the "monopole" magnetic decay length  $c\tau = (2\pi\sigma a^2/c) \ln(b/a)$  becomes much larger than the beam radius  $a$  and the net current is frozen in. Thereafter  $E_z$  takes the value necessary essentially to maintain the value of  $I_b$  established at the pinch point. Since  $\sigma$  is rising rapidly,  $E_z(\zeta)$  decreases rapidly, making the  $E_z$  spike very narrow. Thus, ohmic energy loss extracts energy primarily from beam electrons near the pinch point. Furthermore, ohmic loss results directly in radial expansion, as we have seen. Thus, it is appropriate to regard ohmic loss as primarily a mechanism for erosion of the beam front. If one assumes, for convenience, that the beam current  $I_b(\zeta)$  and voltage  $V$  are constant, then the ohmic energy loss rate is equivalent to erosion of the beam front at a rate [10],[11]

$$d\zeta/dz = (I_n/I_A) \ln(b^2/a^2). \quad (8)$$

We note that nose erosion is additionally driven by scattering, since Nordsieck expansion is fastest at the pinch point, where the pinch force is weak [10]. Scattering-driven erosion is not included in (8).

Calculations [11] also show that if the ionization of the gas is due entirely to beam collisions with gas atoms, then typically  $I_n$  settles down to a slowly varying value

$$I_n = I_b / (1 + \lambda) \quad (9)$$

shortly behind the pinch point. Here  $\lambda = d\tau/dt = d(\pi\sigma a^2/2c)/d\zeta$  is a normalized measure of the beam current. The fractional current neutralization  $f = I_n/I_b$  increases with beam current because  $d\sigma/d\zeta$  is proportional to  $I_b$ ; at higher values of  $I_b$ , the effective current is frozen in at an earlier time. For air, and most other simple gases,  $I_b \sim 10kA$  represents a transition point; higher current beams are mostly current neutralized, while lower current beams are only weakly neutralized.

If  $I_b$  rises to its full value over a time long compared to the temporal delay from the beam head to the pinch point, then the erosion rate and  $I_b$  become functions of the beam rise rate rather than the peak  $I_b$ . However, if the beam propagates far enough, the rising portion of  $I_b(t)$  eventually erodes away and Eqs. (8) and (9) become directly applicable.

Gas Conductivity

We have already had a number of occasions to refer to the evolution of  $\sigma$ , and this aspect of the physics also has a major effect on beam instabilities. At this point, we shall briefly consider the principal mechanisms that underlie plasma conductivity.

The conductivity may be written  $n_e \mu$ , where  $\mu$  is the electron mobility, determined in general by both electron-neutral (e-n) and electron-ion (Spitzer) collisions. Frequently a dense gas is only weakly ionized by a beam and e-n collisions dominate, in which case  $\mu$  is independent of  $n_e$  and only weakly dependent on temperature  $T_e$  (typically,  $\mu \propto 1/T_e$ ). Thus,  $\sigma$  depends primarily on the ionization and de-ionization processes that control  $n_e$ , which increases rapidly from zero to  $n_e > 10^{16}$ . In addition to beam-collisional ionization, avalanche ionization (i.e., ionization of atoms by plasma electrons which have been energized by macroscopic electric fields) may occur, particularly near the pinch point where large electric fields are present. De-ionization is usually due primarily to recombination, at least within the core of the beam. (In some gases, e.g.,  $O_2$ , attachment can be important at large radii or wherever  $n_e$  is relatively low. This will be ignored here.) We may thus write an equation governing the evolution of  $\sigma$ :

$$d\sigma/d\zeta = \alpha_1(T_e) J_b + \alpha_2(T_e) \sigma - \beta(T_e) \sigma^2. \quad (10)$$

In the front portion of the beam and out to one or two beam radii, beam-collisional ionization [the first term of (10)] usually dominates, except possibly at the pinch point. In this case (and if we also neglect the  $T_e$ -dependence) the radial profile of  $\sigma(r)$  is identical to that of  $J_b(r)$ . Moreover, the plasma current  $J(r) = \sigma E_z$  has a similar profile, since  $E_z$  is only weakly dependent on  $r$  within the beam. [See Eq. (11) below.] This approximation is frequently made in analytic studies, and greatly simplifies the analysis. Avalanche [the second term in (10)] has two effects. Avalanche driven by  $E_z$  at the pinch point causes the central  $\sigma(r)$  profile to become narrower than  $J_b(r)$ , a destabilizing effect that will be discussed later. Avalanche driven by  $E_z$  in the very front of the beam produces a very broad low-level conductivity out to the large radius  $b$ , which has important consequences, e.g., the large inductive logarithms in Eq. (8). Further back in the beam, where recombination [the third term of (10)] becomes important,  $\sigma(r)$  becomes broader than  $J_b(r)$ , which helps stability. We note that, in a complex gas such as air, recombination can

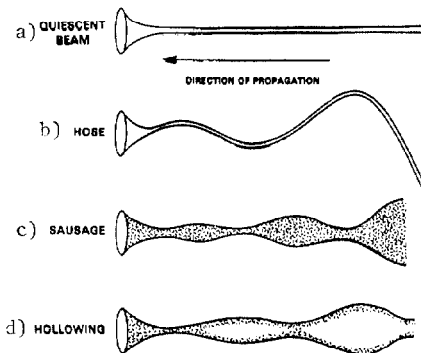
depend on water vapor content and complicated temperature-dependent chemistry effects, e.g., the formation of molecular complexes [12]. On a practical level, even the weak dependence of  $\mu$  on  $T_e$  can have significant effects, e.g., on hose instability [13], as discussed below. To model temperature-dependent effects, it is frequently convenient to assume that (in a diatomic gas)  $T_e$  is determined by a balance between ohmic heating and energy loss to vibrational modes of the molecules. In this case, it can be shown that  $T_e$  is a function only of  $E/\rho$ , where  $E$  is the electric field and  $\rho$  is the gas density. We can then write the coefficients in Eq. (10) as functions of  $E/\rho$ . A summary of these coefficients is given in Refs. 13 and 14.

We have assumed that the plasma conductivity is local, scalar, and is created instantaneously by beam collisions. In fact, beam-gas collisions do create high-energy secondary electrons (delta rays) which have long mean free paths. Although relatively few in number, these secondaries can have some effect in spreading and delaying conductivity, and in responding nonlocally to electric fields. It is also true that tensor conductivity can play some role if the net current is high or the beam radius is small, leading to strong magnetic fields.

### Beam Instabilities

As a magnetically confined, highly ordered system, a self-pinched beam is subject to a number of instabilities, which are driven by two effects: (1) If there is a substantial return current  $I_r = -fI_b$ , then there is a repulsive magnetic force between  $I_b$  and  $I_r$ . As long as  $I_b$  and  $I_r$  remain well aligned and more or less proportional to each other, this merely weakens the pinch in an orderly way, but if perturbations lead to a separation of  $I_b$  and  $I_r$ , the repulsive force can drive unstable growth of the perturbations. This is the primary mechanism for all of the instability modes except hose. Each has a threshold value of  $f$  below which the mode is stable [15]. (The hose mode is unstable even if  $f=0$ , but is further destabilized by non-zero return current.) (2) Even if  $I_r=0$ , symmetry-breaking distortions can drive locally destabilizing magnetic forces. Finite plasma resistivity plays a key role here. Because  $\sigma \neq \infty$ , magnetic field lines are not frozen into the plasma, and instabilities can occur on the time scale for beam motion, rather than the much slower hydrodynamic time scale for the plasma. But because  $\sigma \neq 0$ , the field lines are subject to destabilizing phase lags as they try to follow beam distortions. This mechanism particularly drives the resistive hose instability, which is the most notorious of the beam instabilities.

Fig. 1 BEAM INSTABILITIES



The linearized normal modes of a beam can be characterized by a pair of quantum numbers  $(m,n)$ , where  $m$  indicates  $\theta$ -dependence  $\exp(im\theta)$ , and  $n$  is the radial mode number, roughly speaking the number of oscillations within the beam radius. The first few modes, shown in Fig. 1, are the most important for

pinched beams:  $(m=0,n=1)$  is the sausage mode, roughly a self-similar expansion/contraction of the beam;  $(m=0,n=2)$  is the axisymmetric hollowing mode, in which the beam density alternately hollows out and peaks on axis;  $(m=1,n=0)$  is the hose mode, in which the beam thrashes around more or less like a firehose, without a great deal of internal distortion. The filamentation modes  $(m \geq 2 \text{ or } n \geq 3)$  generally have a high threshold value of  $f$  [15] and are believed to be stable for pinched beams, except in annular (usually rotating) beam equilibria.

### Axisymmetric Hollowing Instability

The axisymmetric hollowing instability was discovered in computer simulations [14] as a particularly violent instability, leading to rapidly growing radial oscillations that destroy the beam only a few nanoseconds behind the pinch point. Computer simulations have provided a detailed, quantitative, and rather surprising picture of its nature. Figure 2 shows the growth of the instability as a function of  $z$  and  $\zeta$  (used as independent variables in place of the usual  $z$  and  $t$ ), and Fig. 3 shows the radial profile  $J_b(r,\zeta)$  characteristic of the instability.

Since the simulations show the instability in the large-amplitude nonlinear stage, where large radial oscillations are apparent, it was thought at first that this was basically a sausage instability, although hollowing of the beam profile is apparent in Fig. 3. However, when the beam profile was constrained to a self-similar shape, the instability disappeared, thus indicating that hollowing is an essential feature. Furthermore, a linearized analytic theory of the sausage mode [16] shows that instability is not expected for a beam injected into neutral gas. [Basically this is because beam perturbations create similar conductivity perturbations through Eq. (10). This effect inhibits spatial separation of  $I_b$  and  $I_r$ , and thus reduces the growth rate for all modes; it just barely suffices to stabilize the sausage mode.] Furthermore, when the avalanche term in Eq. (10) was artificially turned off, the instability disappeared. Finally, it was found that when  $E/\rho$  was extremely large (specified below), the instability turned off.

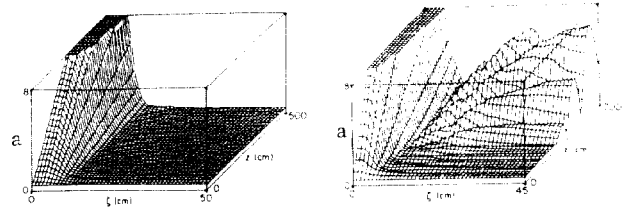


Fig. 2. Beam radius  $a$  as a function of  $z$  and  $\zeta$ , showing the large radial oscillations due to the hollowing instability. (From Ref. 14)

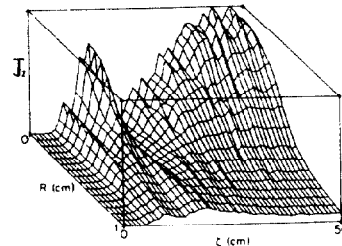


Fig. 3. Beam current density as a function of  $\zeta$  (the distance behind the beam head) for fixed  $z$ , showing hollowing and peaking. (From Ref. 14)

The essence of the hollowing instability is as follows. Behind the pinch point, where Ampere's law (in its axisymmetric form) is valid, one can show that the electric field has the radial profile

$$E_z(r) = \ln[(1+b^2/a^2)/(1+r^2/a^2)]. \quad (11)$$

$E_z$  has a weak (logarithmic) maximum on axis, which is usually ignored in analyses. However, over a wide range of parameters, the exponentiation rate for avalanche ionization rates increase as a high power (4 to 6) of  $E/\rho$ . Thus,  $\sigma$ , and also the plasma return current  $J_r = E_z \sigma$ , become strongly peaked there, and the repulsive magnetic force hollows out the beam and blows it out to large radius. This expansion reverses itself only because the radial expansion of the beam current decreases the inductance  $L$  of the system. Roughly speaking,  $LI$  tends to be constant, so the defocusing plasma current decreases, or may even reverse itself so as to augment the pinch [17,18]. The beam current then comes crashing back onto the axis, and the cycle is repeated with rapidly increasing amplitude.

The key quantitative features revealed by the simulations are that the instability occurs, over a wide range of densities, only if two conditions are met. First,  $f > 50\%$ , in qualitative agreement with prior analytic predictions [15]. This is easily understood: even if the return current flows in a profile that is very narrow compared to the beam current, the pinch is destroyed overall if and only if  $J_r > J_b/2$ . Secondly, the value of  $E_z/\rho$  at the pinch point (in air) must fall into the range

$$13 \text{ MV/m-torr} < E_z/\rho < 50 \text{ MV/m-torr}. \quad (12)$$

The lower limit on  $E_z/\rho$  ensures that avalanche is strong enough to play a significant role. The upper limit is due to the fact that, although avalanche is very strong at large values of  $E/\rho$ , it no longer increases rapidly as a function of  $E/\rho$ .

In order to avoid the hollowing instability, it is thus necessary to keep the maximum value of  $E_z$  below the lower limit of Eq. (12). (In gas at any significant fraction of atmospheric density, the upper limit is not exceeded.) This can be accomplished in several ways: (1) By limiting the rise rate of  $I_b(t)$ , so that the current at the pinch point is not above a critical value. (2) By limiting the peak value of  $I_b$ . Even if  $I_b(t)$  rises instantaneously, instability occurs (in air) only if  $I_b > 20 \text{ kA}$  times the density in atmospheres, for beam radii in the vicinity of 1 cm. (3) Increasing the beam radius.

These conclusions were subsequently tested in an experiment performed on the IBEX electron beam facility at Sandia National Laboratories [19]. The hollowing instability was clearly seen to occur at air densities below 80 torr, in quantitative agreement with predictions based on Eq. (12), and to turn off at higher pressures where  $E_z/\rho$  became too small.

#### Hose Instability

The resistive hose instability is the most important impediment to propagation of pinched beams. It is observed in nearly all beam propagation experiments, and has been studied extensively by means of linearized analytic theory as well as both linearized and nonlinear numerical simulations. The analysis indicates that the instability is always present for a pinched beam injected into neutral gas, but that it can be minimized by limiting the beam duration and reducing the level of initial perturbation.

Analytic studies of the hose instability have usually been based on linearized theory for perturbations to an axially uniform beam equilibrium, i.e.,  $J_{b0}(r, \zeta)$  independent of  $\zeta$ . Hose normal modes take the form  $f(r, \zeta) \exp[i(\theta + \Omega z)/c]$ . It may also be assumed that the equilibrium plasma current  $J_{p0}(r, \zeta)$  and (in the simpler theories) conductivity  $\sigma_{p0}(r, \zeta)$  are  $\zeta$ -independent, in which case the normal mode dependence reduces to  $f(r) \exp[i(\theta c + \omega \zeta + \Omega z)/c]$  and a

dispersion relation  $\omega(\Omega)$  is sought. Effects associated with the beam head and pinch point, e.g., low conductivity, space charge, and incomplete pinch, are usually neglected, and in this spirit the electro-dynamics are calculated simply from Ampere's law (exceptions are Refs. 20,21).

The earliest version of hose theory (the "rigid beam" model) assumed in addition that the perturbation of each "slice" of the beam consists of a transverse displacement by an amount  $Y \exp[i(\omega \zeta + \Omega z)]$ , with no internal distortion. As a nearly exact consequence of the linearized Ampere's law the vector potential  $A_z(r, z, \zeta)$  is also displaced from the axis of symmetry, by an amount  $D \exp[i(\omega \zeta + \Omega z)]$ , without internal distortion. The problem reduces to ODE's,

$$\partial^2 Y / \partial z^2 = \Omega_\beta^2 (D - Y) / c^2 \quad (13)$$

$$D + c \tau_1 (\partial D / \partial \zeta) = Y, \quad (14)$$

where  $\tau_1 = \pi \sigma a^2 / 2c^2$  is the "dipole" magnetic decay time. Equations (13) and (14) lead to a dispersion relation

$$i \omega \tau_1 = -\Omega^2 / (k_\beta^2 - \Omega^2), \quad (15)$$

which correctly shows that oscillation in  $z$  scales to  $\lambda_\beta$  while growth in  $\zeta$  scales to the  $\tau_1$ . However, the infinite growth rate predicted at  $\Omega = k_\beta$ , indicative of absolute instability in the beam frame, is incorrect.

The crucial oversimplification in Eqs. (13)-(15) is the implicit assumption that all beam electrons oscillate at a single resonant betatron frequency, i.e., that the potential well pinching the beam is simply harmonic. This would be true for a flat-topped current profile, but the rounded profiles of  $J_b$  and  $J_r$  introduce anharmonicity, and therefore a dependence of  $k_\beta$  on the amplitude of an electron's orbit. When this feature is introduced into the modeling, as was first done by using the "spread mass" formalism [22], the dispersion relation exhibits a finite maximum growth rate. For example, Lee [22] finds

$$-i \omega \tau_1 = 3x^2 - 6x^4 + 6(x^4 - x^6)[i\pi + \ln(1/x^2 - 1)], \quad (16)$$

where  $x = \Omega^2 / \Omega_\beta^2$ . Equation (16) is illustrated in Fig. 4, for a beam with no return current. Most significantly, the instability is convective backward in the beam frame; hence, it reaches a maximum amplitude at any given point in the beam and then decays. Thus, the hose amplitude can be limited by limiting the beam duration to a few growth lengths and by insuring that the beam is initially quiescent, so that hose modes have to e-fold many times.

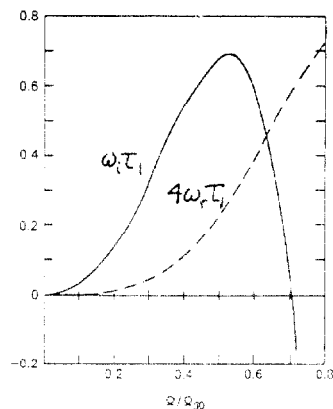


Fig. 4. Dispersion relation for hose instability from the spread mass model.

Subsequent to Lee's pioneering work, hose modeling has been extended in many ways. More sophisticated macroscopic models [23], linearized Vlasov calculations [24], and simulations [17],[18],[23]-[25] have been used to treat beam dynamics. Plasma return current has been included and found to be strongly destabilizing [23],[24],[26]. Self-consistent treatment of conductivity evolution introduces a variety of effects. A fully analytic linear theory has been developed which includes the linear increase of equilibrium conductivity  $\sigma(r,\zeta)$  with  $\zeta$  due to beam-collisional ionization of the gas; in this case, instability grows as a power  $p$  of  $\zeta$ , rather than exponentially [24]. Since  $p$  is inversely proportional to  $\sigma$ , growth is most rapid just behind the pinch point. (The formalism is invalid ahead of the pinch point). Furthermore, dipole perturbations of the beam induce dipole perturbations of  $\sigma$  through Eq. (10). This significantly reduces the growth rate in the presence of plasma return current, particularly for low frequency modes, by inhibiting separation of the beam current from the return current [24]. One consequence of this is that the hose growth rate typically decreases with increasing  $I_b$ , as shown in Fig. 5. This is the net result of three pieces of physics: (i)  $\tau_1 \propto I_b$ , which favors higher currents; (ii) the destabilizing effect of current neutralization favors lower currents; (iii) the effect of dipole conductivity swings the balance to higher currents. Even the  $T$ -dependence of  $\sigma$ , i.e., the inverse dependence of  $\sigma$  on  $E/\rho$ , can be included in a fully analytic theory [13]; since  $E_z$  is largest at the pinch point and steadily decreases thereafter, this further accentuates the tendency for hose to grow rapidly at the pinch point and very slowly further back in the beam.

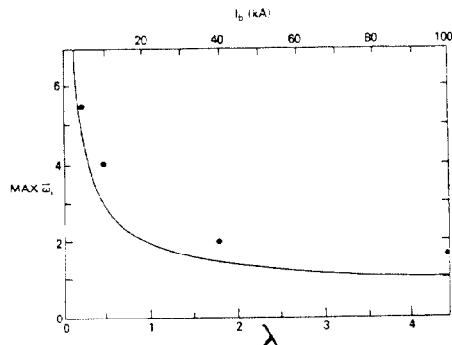


Fig. 5. Peak hose growth rate as a function of beam current. (From Ref.24)

Numerical simulation has been essential to detailed understanding of hose [17],[18],[24],[25]. It permits self-consistent treatment of the radial and  $\zeta$  dependence of beam equilibria, of phenomena near the pinch point where Ampere's law is invalid, and of nonlinear effects. Conversely, the hose instability has stimulated the development of an innovative simulation model [24],[25]. One conclusion from these studies is that avalanche ionization at the pinch point is lethal, strongly driving hose as well as axisymmetric hollowing, and for similar reasons.

#### Conclusions

We have seen that propagation of beams in dense gases is limited in varying ways by energy loss, radial expansion, nose erosion, and hose and hollowing instabilities. For the most part, these limitations are minimized by going to higher energies and currents, fatter beams, shorter pulses, and beams which are more quiescent at injection.

#### References

[1] E. P. Lee, Lawrence Livermore National Laboratory Report UCID-18940, 1981.

[2] J. D. Jackson, *Classical Electrodynamics*, New York: Wiley, 1967, pp. 440,458, 519.

[3] B. Rossi, *High Energy Particles*, Englewood Cliffs, N. J.: Prentice-Hall, 1952, p. 55.

[4] M. I. Haftel, M. Lampe, and J. B. Aviles, *Phys. Fluids* 22, 2216-2229, 1979.

[5] E. P. Lee, *Phys. Fluids* 19, 60, 1976.

[6] E. P. Lee and R. K. Cooper, *Part. Accel.* 7, 83, 1976.

[7] H. A. Bethe, *Phys. Rev.* 89, 1256, 1953.

[8] T. P. Hughes and B. B. Godfrey, *Phys. Fluids* 27, 1531, 1984.

[9] R. J. Briggs, R. E. Hester, E. J. Lauer, E. P. Lee, and R. I. Spoerlein, *Phys. Fluids* 19, 1007, 1976.

[10] E. P. Lee, Lawrence Livermore National Laboratory Report UCID-18768, 1980.

[11] W. M. Sharp and M. Lampe, *Phys. Fluids* 23, 2383, 1984.

[12] A. W. Ali, NRL Memo Report 4617, 1981.

[13] S. P. Slinker, R. F. Hubbard, and M. Lampe, "Variable Collision Frequency Effects on Hose and Sausage Instabilities," NRL Memo Report (in press).

[14] G. Joyce and M. Lampe, *Phys. Fluids* 26, 3377, 1983.

[15] H. S. Uhm and M. Lampe, *Phys. Fluids* 25, 1444, 1982.

[16] M. Lampe and G. Joyce, *Phys. Fluids* 26, 3371, 1983.

[17] B. Hui, R. F. Hubbard, M. Lampe, Y. Y. Lau, R. R. Fernsler, and G. Joyce, *Phys. Rev. Lett.* 55, 87, 1985.

[18] R. F. Fernsler, R. F. Hubbard, B. Hui, G. Joyce, M. Lampe, and Y. Y. Lau, *Phys. Fluids* 29, 3056, 1986.

[19] C. A. Ekdahl, J. R. Freeman, G. J. Leifeste, R. B. Miller, W. B. Styger, and B. B. Godfrey, *Phys. Rev. Lett.* 55, 935, 1985.

[20] E. P. Lee, Lawrence Livermore National Laboratory Report UCID-16734, 1975.

[21] H. S. Uhm and M. Lampe, *Phys. Fluids* 24, 1553, 1981.

[22] E. P. Lee, *Phys. Fluids* 21, 1327, 1978.

[23] W. M. Sharp, M. Lampe, and H. S. Uhm, *Phys. Fluids* 25, 1456, 1982.

[24] M. Lampe, W. M. Sharp, R. F. Hubbard, E. P. Lee, and R. J. Briggs, *Phys. Fluids* 27, 2821, 1984.

[25] G. Joyce and M. Lampe, *J. Comp. Phys.* 63, 398, 1986.

[26] H. S. Uhm and M. Lampe, *Phys. Fluids* 23, 1574, 1980.

\*Work supported by DARPA under Contract No. N60921-86-WR-W0233, ARPA Order No. 4395, Amendment 63.